Photoemission study of onion like carbons produced by annealing nanodiamonds

Journal Item

Photoemission study of onionlike carbons produced by annealing nanodiamonds

Yu. V. Butenko,[1,2,*] S. Krishnamurthy,[1] A. K. Chakraborty,[3,4] V. L. Kuznetsov,[2]
V. R. Dhanak,[5,6] M. R. C. Hunt,[3] and L. Šiller[1]
[1]*School of Chemical Engineering and Advanced Materials, The University of Newcastle upon Tyne, Newcastle upon Tyne, NE1 7RU, United Kingdom*
[2]*Boreskov Institute of Catalysis, Lavrentieva 5, Novosibirsk, 630090, Russian Federation*
[3]*Department of Physics, The University of Durham, Durham, DH1 3LE, United Kingdom*
[4]*School of Physics & Astronomy, The University of Nottingham, Nottingham, NG7 2RD, United Kingdom*
[5]*CCLRC, Daresbury Laboratory, Warrington, Cheshire, WA4 4AD, United Kingdom*
[6]*Surface Science Centre, Liverpool University, Liverpool, L69 3BX, United Kingdom*
(Received 28 June 2004; revised manuscript received 11 October 2004; published 25 February 2005)

Photoelectron spectroscopy has been used to study the products resulting from high temperature phase transformation of nanodiamonds (ND). Depending on the temperature of annealing various particles with a diamond core covered by nanometer sized fullerene-like shells, and onionlike carbon (OLC) were formed. Analysis of the C1*s* photoemission lines of the intermediates of ND transformation, prepared at temperatures of 1420 and 1600 K and then exposed to atmosphere, reveals the presence of oxygen-containing groups and both sp^2 and sp^3 carbon. The sp^2 component for these samples has binding energies of 284.70 ± 0.05 eV (for the sample prepared at 1420 K) and 284.50 ± 0.05 eV (for the sample prepared at 1600 K). A difference of 1.3 ± 0.1 eV in the binding energy of the sp^3 and sp^2 components was observed. The sp^2 component for OLC prepared at 1800, 1900, and 2140 K has a binding energy of 284.45 ± 0.05 eV. The shift towards higher binding energies of the sp^2 component of the samples prepared at lower temperatures is explained by significant curvature of graphite layers formed in the initial stages of graphitization. The observed increase in density of states at the Fermi level for the samples prepared at 1600, 1800, and 1900 K is associated with an accumulation of different types of defects in the curved graphite layers during graphitization of diamond. The Lorentzian widths of C1*s* photoemission lines from OLC are large compared with those of HOPG. The possible reasons for this broadening are discussed.

DOI: 10.1103/PhysRevB.71.075420 PACS number(s): 73.61.Wp, 73.20.Hb, 79.60.Jv, 68.43.Vx

I. INTRODUCTION

Carbon onions consist of fullerenelike shells enclosed within one another (multishell fullerenes) and belong to the family of carbon nanostructures. The first observation of carbon onions was in arc discharge products[1] and later in fullerene soot irradiated by an intense electron beam.[2] Carbon onions are predicted to have properties different from those of graphite, diamond and other carbon nanostructures (such as carbon nanotubes) due to their highly symmetric structure.[3] In depth investigation of the physico-chemical properties of this unique carbon form and exploration of possible applications was constrained until recently by the absence of methods allowing production of carbon onions with a well-ordered structure in sufficiently large quantities.

Carbon onions have been produced by the transformation of different carbon nanostructures.[2,4–7] Carbon onions produced by electron irradiation of a carbon nanomaterial have a perfect spherical form and well ordered structure, but due to the small rate of production they can be studied only by high-resolution transmission electron microscopy (HRTEM) and electron energy loss spectroscopy (EELS).[8] De Heer and Ugarte[9] demonstrated the possibility of producing macroscopic quantities of onionlike carbon (OLC) consisting of hollow carbon onions with from 2 to 8 graphitic shells and with outer diameters ranging from 3 to 10 nm by heating carbon soot, produced by an arc-discharge method, in vacuum at 2100–2250 °C. Raman spectra of this material revealed pronounced differences to other graphitic materials.[10] Cabioc'h *et al.*[11–13] developed a method of carbon onion production (with typical diameters in the range 3–15 nm) based on carbon ion implantation into a metal matrix (Ag, Cu). Sufficient quantities could be produced for investigation of their optical, electronic and tribological properties.[14–17] These carbon onions were characterized by Fourier transform infrared (FTIR) spectroscopy[16] and it was shown that the most stable state for the onions consists of concentric spheres of fullerenes C_n ($n=60, 240, \ldots$). Until now, the electronic properties of the onions were characterized only by spatially resolved EELS in transmission[15,18] and reflection mode.[19]

Recently Sano *et al.*[20–22] reported the production of several milligrams of carbon onions with diameters ranging from 4 to 36 nm using an arc discharge between two graphite electrodes submerged in water or liquid nitrogen. It has been shown that depending upon synthesis conditions the carbon nanoparticles produced by this method contain carbon onions with a perfect spherical shape along with defective carbon onions and a minimum amount of amorphous carbon and carbon nanotubes. These carbon onions have been characterized by Raman spectroscopy[23] and by ultraviolet-visible absorption spectroscopy.[24] New Raman peaks were observed in spectra of the carbon onions compared with a Raman spectrum from highly oriented pyrolytic graphite (HOPG). The appearance of these new features was explained by the cur-

vature of the graphitic walls of the carbon onions.[23]

Kuznetsov *et al.*[25,26] developed a process for generating several grams of OLC based on annealing nanodiamonds (ND), with sizes in the range 2–20 nm, in vacuum. It has been shown that, depending upon temperature and duration of ND annealing, different forms of OLC can be produced. Annealing ND for one hour at (a) 1100–1600 K produces spiral-like multishell carbon particles with structures being intermediate in the transformation from sp^3 to sp^2 carbon. These consist of ND particles covered with nanometer sized fullerenelike shells, which are similar to so called "bucky diamonds;"[27,28] (b) 1800–1900 K leads to the formation of OLC containing the maximum concentration of carbon onions with 3–8 fullerenelike spherical shells and aggregates of onions with extended curved graphitic layers between them; (c) above 2100 K leads to the formation of larger polygonal hollow onions with a structure similar to that which was observed when fullerene-containing soot was annealed at temperatures above 2300 K.[9,29]

Since OLC was synthesized in macroscopic quantities, it has become possible to explore its physical and chemical characteristics. It has been shown that due to an efficient optical limiting action of OLC, they are good candidates for photonic applications.[30] OLC also demonstrates high selectivity and catalytic activity in the oxidative dehydrogenation of ethyl benzene to styrene.[31] The properties of OLC produced by annealing ND have been investigated by x-ray emission spectroscopy,[32] Raman spectroscopy,[33] electron energy-loss spectroscopy,[34] electron-spin resonance,[35] x-ray diffraction,[36] and ultraviolet-visible absorption spectroscopy.[37] A photoemission study of potassium intercalated polygonal hollow onions produced at 2140 K showed that these carbon onions behave as small graphite crystals and hence display bulklike rather than molecularlike behavior.[38] The x-ray emission study of OLC produced in the temperature range of 1600–1900 K revealed that their C K_α spectra exhibit a significant increase of the high-energy maximum and are markedly different from the spectrum of particles formed at 2140 K, which is very similar to the C K_α spectrum of polycrystalline graphite.[32] However, due to dipole selection rules, the x-ray emission spectra yield information on the partial density of states. Until now, the full electronic structure of OLC has not been studied. In this work we present results of a photoemission study of OLC produced by annealing ND in vacuum in the temperature range 1100–2140 K. Photoemission spectroscopy is an ideal method for measuring the (matrix element weighted) full density of states. In particular, it is interesting to monitor changes in electronic structure of these samples during progressive graphitization and consequent reduction of the sp^3/sp^2 carbon ratio.

II. EXPERIMENT

Samples of nanodiamond (ND) were produced through explosion and isolated from the detonation soot by oxidative treatment with a mixture of $HClO_4$ and H_2SO_4.[39] According to small-angle x-ray scattering (SAXS) and HRTEM studies the size of ND particles varies from 2 to 20 nm with an average particle size of 4.7 nm.[26] The various samples studied in this work were prepared by high temperature annealing of the ND under a vacuum of 10^{-5} Torr for 1–1.5 h at the temperatures mentioned above, as described elsewhere.[26]

X-ray photoelectron spectroscopy (XPS) was performed using the ESCA 300 photoelectron spectrometer at the National Centre for Electron Spectroscopy and Surface Analysis (NCESS), Daresbury Laboratory, UK. The samples were deposited by dropping an isopropanol suspension of the ND onto a sample cut from a silicon wafer with a native oxide layer. Samples were also produced by depositing an isopropanol suspension of the OLC and annealed ND intermediates directly onto a stainless steel sample holder. The samples were then left to dry for several hours in air. The fresh, clean HOPG (0001) surfaces were prepared by cleaving the sample with a tape in air followed by immediate insertion of the sample into an ultra high vacuum (UHV) chamber. After insertion into UHV, C1*s* spectra of the carbon specimens were measured in normal emission geometry using monochromated Al K_α radiation (photon energy 1486.6 eV). An overall energy resolution 0.39 eV was determined from the Gaussian width of the C1*s* line of HOPG. All measurements were carried out at a pressure in the 10^{-9} Torr range. A flood gun was only used to irradiate the initial ND sample and ND annealed at 1170 K with 1 eV electrons in order to compensate for charging effects in the insulating diamond samples.

Valence-band spectra were acquired at Beamline 4.1 of the Synchrotron Radiation Source (SRS) at Daresbury Laboratory, U.K. Experiments were carried out in an ultra-high vacuum chamber with a base pressure in the 10^{-10} Torr region. The samples were prepared by dropping isopropanol suspensions of OLC or ND intermediates onto substrates cut from a silicon wafer with a native oxide layer. After drying, the silicon plates were mounted in a sample holder in which the OLC or ND intermediate film was in a good electrical contact with tantalum retaining clips. Before the measurements of valance band spectra the samples were annealed at 1300 K for 5 minutes to remove adsorbates such as condensed water, traces of isopropanol and oxygen-containing groups. Photoemission spectra were measured in normal emission geometry using a SCIENTA SES-200 analyzer and a photon energy of 55 eV. The binding energy scales of the valence-band spectra were calibrated by measuring the position of the Fermi edge obtained from a platinum foil in good electrical contact with the sample. An overall energy resolution 0.20 eV for the valence band was determined from the width of the Fermi cutoff.

The C1*s* photoemission spectra of sp^2 bound carbon were fitted using a Doniac-Šunjić line shape[40] convoluted with a Gaussian. The Gaussian component accounts for the instrumental energy resolution together with any chemical disorder, and the Lorentzian width accounts for the finite core hole lifetime associated with the photoionization process. The sp^3 bound carbon component, components corresponding to carbon atoms bound to oxygen and the π plasmon peak were all fitted with Lorentzian peaks convoluted with the same Gaussian employed for broadening the sp^2 related peak. The background photoelectron intensity was subtracted by the Shirley method.[41]

TABLE I. Physical characteristics of OLC samples prepared at different temperatures.

Annealing temp. (K)	570	1170	1420	1600	1800	1900	2140
Density (g/cm^3) (Ref. 26)	3.11 ± 0.02	3.07 ± 0.02	2.90 ± 0.02	2.53 ± 0.02	2.14 ± 0.02		2.03 ± 0.02
Diamond fraction (Ref. 26)			0.86 ± 0.05	0.57 ± 0.05	0.15 ± 0.05		0
Electrical resistivity At room temp. (Ω cm) (Ref. 42)	$>10^9$	$>10^9$	$160\pm2\times10^3$	0.50 ± 0.02	0.20 ± 0.02	0.30 ± 0.02	0.18 ± 0.02

III. RESULTS

Table I presents some of the physical characteristics of the ND samples prepared at different temperatures, which were obtained in our previous work.[26,42] The values of the diamond fraction of the samples annealed at 1420, 1600, and 1800 K presented in the table were estimated from the values of their density. According to HRTEM data and measurements of the sample densities, the graphitization of ND starts at temperatures above 1400 K.[26] The graphitization under annealing begins from the surface and proceeds towards crystal bulk.[25,43,44]

Figure 1 presents HTRTEM images and schematic diagrams of the products of graphitization of ND. The schematics summarize the results of our previous HRTEM investigations of OLC and intermediates of ND to OLC transformation.[25,26,32,43] Due to the strong aggregation of the initial particles of ND the resulting OLC (shown in the schematic for annealing to 1800–1900 K) mostly consist of aggregates of carbon onions. OLC particles are connected together by joint curved graphite layers. According to HRTEM images one carbon onion can have up to 5 neighboring onions joined to it by the curved graphite layers. The difference in crystal structure of diamond and graphite results in an accumulation of different types of defects in the graphite curved layers during their formation from diamond carbon. Among these defects "Y" junctions of two basal graphite planes and interstitial planes between two basal planes are clearly observed in HRTEM images. The "Y" junctions in HRTEM images can reflect, along with the presence of real "Y" junctions between graphene sheets, the presence of spiral-like structures, which can be observed in OLC. It is interesting to note that the formation of spiral-like carbon structures has been observed in different processes. Kroto and McKay[45] proposed the growth of the spiral shell carbon particles during the condensation of carbon vapor. Ozawa *et al.*[46] showed the formation of 3D spiral carbon particles in a furnace black irradiated by an electron beam. According to

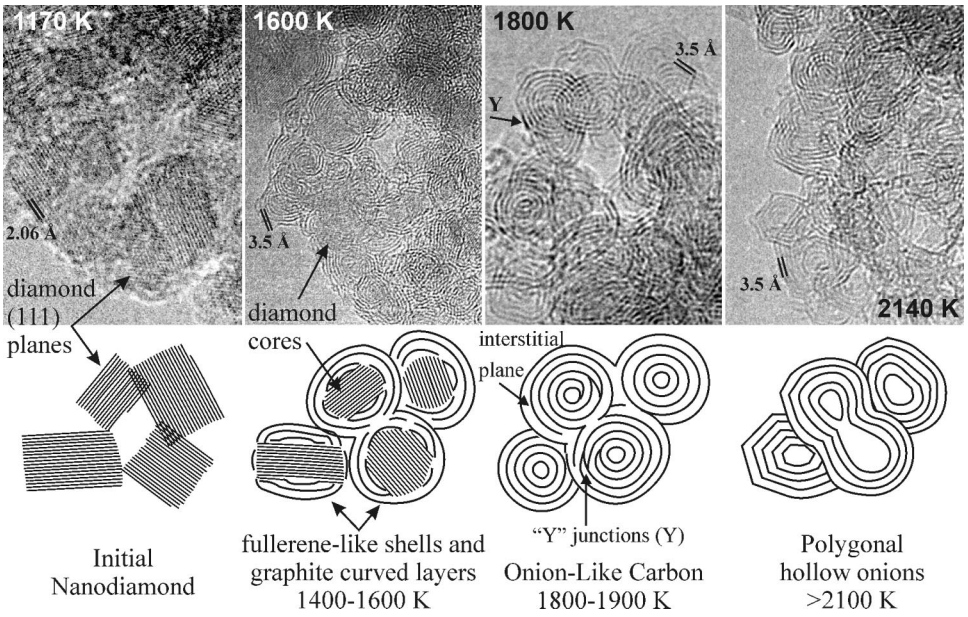

FIG. 1. HRTEM images and schematic diagrams of the products of ND graphitization at different temperatures (shown on the images). The figure summarizes our HRTEM data on the structures OLC and intermediates of ND to OLC transformation. (Refs. 25, 26, 32, 39, and 43). The straight dark lines on the HRTEM images and the schematic of the initial ND and the intermediates of ND transformation at 1400–1600 K correspond to (111) planes of diamond with interplanar distance of 2.06 Å. Curved solid lines correspond to (0002) graphitelike layers with an interplanar distance of approximately 3.4–3.6 Å. These crystallographic planes of diamond and graphite are clearly seen on the HRTEM images. Annealing at 1800–1900 K leads to the formation of OLC containing the maximum concentration of carbon onions with 3–8 fullerenelike spherical shells and aggregates of carbon onions. Annealing above 2100 K leads to the formation of polygonal hollow onions.

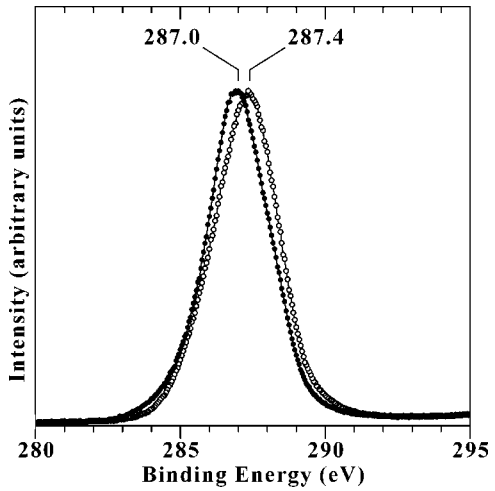

FIG. 2. C1*s* photoemission spectra of ND annealed in vacuum at 570 K (open circles) and at 1100 K (full circles) and then exposed to atmosphere. The spectra were obtained in normal emission geometry at a photon energy of 1486.6 eV.

our HRTEM observations the major part of the OLC particles contain from 3 to 8 fullerenelike shells. OLC particles containing 9–20 shells have a polygonal structure, no larger particles were observed. Concentration of the larger OLC particles is very low. Defects are annealed out at temperatures above 2100 K, however, in this case, the structure of carbon onions changes to hollow polygonal onions.

Figure 2 presents the C1*s* photoemission spectra of initial ND (open circles) and ND annealed at 1170 K (full circles) and then exposed to atmosphere. The spectra were normalized with respect to peak height. The C1*s* peak of the initial ND has a maximum at 287.4 ± 0.1 eV and a full width at half maximum (FWHM) of 2.65 ± 0.05 eV while the C1*s* peak of the ND annealed at 1170 K has maximum at 287.0 ± 0.1 eV with FWHM of 2.55 ± 0.05 eV. We observed the presence of oxygen (an O1*s* line, not shown here, could be observed) at substantial concentrations in both samples, indicating that oxygen-containing groups exist on the diamond surface. Wilson *et al.*[47] found that the C1*s* peaks of oxygen-containing groups are shifted to higher binding energy from the main sp^3 component by 1.2–1.6 eV for ether ($\geqslant$C-O-C$\leqslant$) groups and by 2.6–2.9 eV for carbonyl ($>$C=O) groups. In both the C1*s* spectra from ND these peaks are not resolved (Fig. 2), but they lead to a broadening of the spectra.

Oxygen-containing groups, such as $\geqslant$C-OH (hydroxyl), $\geqslant$C-O-C$\leqslant$ (ether), $>$C=O (carbonyl), -COOH (carboxyl), -C(O)OC$\leqslant$ (ester),[48] were formed on the surfaces of the ND starting material during oxidative treatment in the $HClO_4$ and H_2SO_4 mixture. According to temperature programmed desorption (TPD) data, thermal decomposition in vacuum of these different groups occurs at different temperature ranges and finishes at a temperature of 1100 K.[48] The presence of oxygen-containing groups on the surface of the sample annealed at 1170 K is explained by exposure to air after the annealing. The 0.4 eV shift between the spectra can be explained by the different composition of oxygen-containing groups on the initial ND sample and the sample annealed at 1170 K and subsequently exposed to atmosphere, which

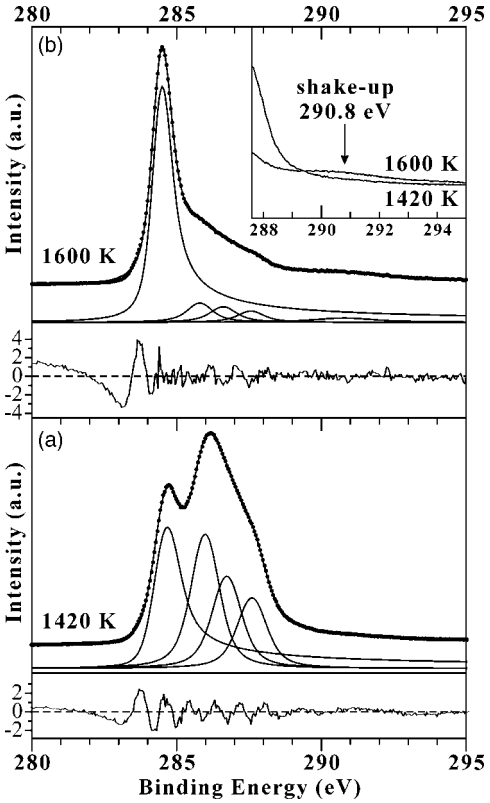

FIG. 3. C1*s* photoemission spectra of ND annealed at (a) 1420 K and (b) 1600 K and then exposed to atmosphere. The spectra were obtained in normal emission geometry at a photon energy of 1486.6 eV. The dots are experimental data and the solid lines are the fit components into which the spectra were decomposed; the background is subtracted by the Shirley method. The resulting fit is superimposed on the data. The inset shows the appearance of the π plasmon peak (shakeup) at 290.8 eV in the spectrum of the sample annealed at 1600 K. The residuals from the curve fitting (in units of standard deviation) are displayed in the bottom panel beneath the spectra.

arises from the differences between their preliminary treatments. It is interesting to note that previous HRTEM studies did not reveal the presence of well-ordered graphitic structures on the surface of the sample annealed at 1170 K (see Fig. 1).[26,42] The absence of a pronounced sp^2 component at lower binding energy in the C1*s* photoemission spectrum (Fig. 2) of this sample also indicates that the annealing of ND at 1170 K is insufficient to produce appreciable graphitization.

Figure 3(a) shows the C1*s* photoemission spectrum of ND annealed at 1420 K together with the corresponding fit curves. The spectrum contains a clearly resolved peak at 284.7 ± 0.1 eV. We assign this peak to sp^2 carbon because the C1*s* line in graphite occurs at lower binding energy than that in diamond.[49] However, this value of binding energy is 0.3 eV larger than values previously reported for the C1*s* binding energy in graphite.[50,51] The possible reasons for this difference will be discussed in the next section. We attribute the peak at 286.10 ± 0.05 eV binding energy with a pronounced shoulder at higher binding energy to sp^3 bound carbon and carbon bound to different oxygen-containing groups. Even

TABLE II. C1*s* line shape parameters determined from fits to experimental data obtained from ND annealed at 1420 K and 1600 K (Fig. 3).

Fit parameters		ND annealing temperature K 1420	1600
sp^2 component	Binding energy (eV)	284.70±0.05	284.50±0.05
	FWHM (eV)	1.2±0.1	0.9±0.1
	Singularity index (α)	0.22±0.02	0.17±0.01
	Fractional peak area (%)	48±2	85±2
sp^3 component	Binding energy (eV)	286.0±0.1	285.8±0.1
	FWHM (eV)	1.2±0.1	1.1±0.1
	Fractional peak area, (%)	23±2	4.9±0.3
⩾C-OH, ⩾C-O-C⩽	Binding energy (eV)	286.7±0.1	286.6±0.1
	FWHM (eV)	1.2±0.1	1.1±0.1
	Fractional peak area (%)	17±1	4.2±0.3
>C=O	Binding energy (eV)	287.6±0.1	287.6±0.1
	FWHM (eV)	1.2±0.1	1.2±0.1
	Fractional peak area (%)	12±1	3.0±0.3
π plasmon peak	Binding energy (eV)		290.8±0.1

though graphitization occurs initially at the surface of the ND, we can observe the sp^3 component because the electron escape depth is several nanometers,[52] and thus larger than the thickness of the 1–3 graphitic layers present on the diamond surface determined by HRTEM (distance between the graphitic layers in the samples is approximately 0.34-0.35 nm).[26]

As mentioned above, in contrast with the sample annealed at 1170 K, the surface of ND annealed at 1420 K is covered by curved graphitic layers, which can be clearly seen by HRTEM (see Fig. 1). In the literature the typical values of shifts in the C1*s* binding energy for carbon bound to oxygen, compared with the main C1*s* peak for graphitic materials, fall into three regions depending on the nature of oxygen-containing groups:[53–58] (1) 1.3–2.4 eV for hydroxyl (⩾C-OH) and ether (⩾C-O-C⩽) groups; (2) 2.6-3.5 eV for carbonyl groups (>C=O); (3) 4.3-5.4 eV for carboxyl (-COOH) and ester (-C(O)OC⩽) groups. Due to the overlap of the sp^3 carbon component with components associated with oxygen-containing groups it is difficult to determine how many types of oxygen-containing groups are present. Therefore we first fitted the region at higher binding energy with one component for sp^3 carbon and with differing numbers of components for oxygen-containing groups (from one to three). The fitting with one component for oxygen-containing groups gave a 1.5±0.1 eV difference in the binding energy of the sp^2 and sp^3 components, which is significantly larger than the differences of 0.9 eV reported for amorphous carbon[49,59] and 0.8 eV for diamondlike-carbon films.[51,60] Therefore, we excluded this fit from our consideration.

Fitting with two and three components for oxygen-containing groups gave a good agreement with the experimental spectra. We found that the position of sp^3 component does not significantly depend on whether we fit two or three peaks associated with oxygen-containing groups, to within experimental error. However, the shift of the peak for carboxylic and ester groups did not correspond to typical literature values when the fitting was performed with three components for oxygen-containing groups. Therefore, we excluded fits with three oxygen-containing groups from the consideration and fitted the spectrum with an sp^3 component at 286.0±0.1 eV and two components, which we assigned to ⩾C-OH and ⩾C-O-C⩽ groups at 286.7±0.1 eV, and >C=O groups at 287.6±0.1 eV. The final fitting parameters for the spectrum of the sample annealed at 1420 K are presented in Table II.

We observed a 1.3±0.1 eV difference in the binding energy of the sp^3 and sp^2 components, which is larger than values obtained with lower resolution: 0.9 eV for amorphous carbon[49,59] and 0.8 eV for diamondlike films.[51,60] The reasons for such a large separation between the two components are not clear, however, fitting with a smaller difference in binding energy did not give a good agreement with the experimental spectrum. A similar separation between sp^2 and sp^3 components was found in Ref. 49 for an amorphous carbon film annealed above 1200 K.

Figure 3(b) presents the C1*s* photoemission spectrum and fit curves of ND annealed at 1600 K. The main peak of the sp^2 component is located at a binding energy of 284.50±0.05 eV. The spectrum contains at least two pronounced shoulders at higher binding energy. The spectrum was fitted with a peak associated with sp^3 bound carbon at 285.8 eV, with a position which was fixed at 1.3 eV from the sp^2 component (found from fitting of the spectrum of the sample annealed at 1420 K), and peaks due to ⩾C-OH or ⩾C-O-C⩽ groups at 286.6±0.1 eV, and >C=O groups at 287.6±0.1 eV. The fitting parameters for the spectrum are presented in Table II.

The singularity index for the sample annealed at 1420 K is 0.22±0.1 which is similar to that which was obtained in Ref. 49 for amorphous carbon films annealed at 1450 K. Further annealing at 1600 K results in a decrease of the sin-

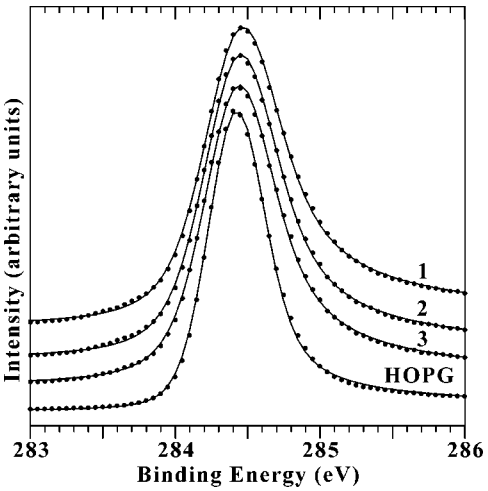

FIG. 4. C1*s* photoemission spectra of ND samples as a function of annealing temperature: (1) 1800 K, (2) 1900 K, and (3) 2140 K, compared with a spectrum obtained from HOPG. The dots are experimental data and the solid lines are resulting fits. The background is subtracted by the Shirley method. The spectra were obtained in normal emission geometry at a photon energy of 1486.6 eV.

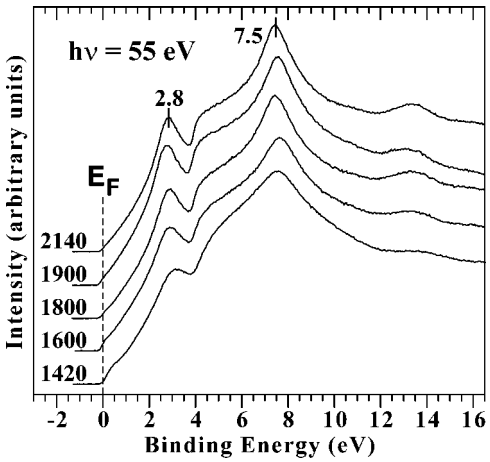

FIG. 5. Evolution of valance band spectra as a function of annealing temperature for samples annealed at 1420, 1600, 1800, 1900, and 2140 K (temperatures on the figure are presented in kelvin). Spectra were obtained in normal emission geometry using a photon energy of 55 eV and spectra were normalized to the total photoemission intensity between −1 eV and 10 eV binding energy

gularity index to 0.17±0.01. The π plasmon peak (shake up satellite), which is associated with π-π^* transitions in graphitic materials,[61] appears at 6.3±0.4 eV from the C1*s* sp^2 peak in the spectrum of the sample annealed at 1600 K. This peak was not observed for the sample annealed at 1420 K (see the inset in Fig. 3).

Figure 4 presents C1*s* photoemission spectra of samples annealed at 1800, 1900, and 2140 K together with a spectrum from HOPG. Analysis of O1*s* photoemission spectra of the annealed ND and HOPG shows that negligible oxygen concentration (less than 0.5%) is present in the samples. Thus, for the spectra in Fig. 4 we did not include the oxygen containing groups in the fitting. The best fits were obtained with one component, for sp^2 carbon. The C1*s* spectra of these materials also contain π plasmon peaks at 290.7±0.4 eV for all OLC and 291.5±0.4 eV for HOPG. The fitting parameters of these spectra are presented in Table III. We found a singularity index in the samples annealed at 1800, 1900, and 2140 K of 0.15±0.1 which is larger than that of 0.11±0.1 for HOPG. The value of the singularity index we obtained for HOPG is lower than the value of 0.14 measured for HOPG in Ref. 46 at lower instrumental resolution. The possible reasons for the larger value of the singularity index in the OLC will be discussed later.

The absence of sp^3 carbon in the sample is consistent with our previous HRTEM data, which showed the absence of diamond structures in samples heated above 1800 K.[26] However, measurement of sample densities revealed the presence of sp^3 carbon in the sample annealed at 1800 K (see Table I). This discrepancy is explained by the presence of sp^3 carbon only in the core of the largest particles (with size up to 20 nm). The "screening" of these diamond cores by surrounding graphite-like shells is the reason for the absence of an sp^3 bound carbon component in the C1*s* XPS spectra of the sample annealed at 1800 K (photoelectrons from the cores have a mean free path shorter than the thickness of the outer graphitic shells). One can suggest that this "screening" effect can alter the relative peak areas of sp^2 and sp^3 components in the C1*s* XPS spectra of the samples annealed at 1420 and 1600 K (see Table II), which will result in values which differ from the sp^2/sp^3 ratios estimated from values of densities of the samples (Table I).

Figure 5 presents valence band spectra of samples annealed at the five different temperatures. The spectra were normalized to the total photoemission intensity between −1 eV and 10 eV binding energy. The spectra contain two

TABLE III. C1*s* line shape parameters determined from fits to experimental data obtained from ND annealed at 1800, 1900, and 2140 K, and HOPG (Fig. 4).

Fit parameters for	ND annealing temperature (K)			
sp^2 component	1800	1900	2140	HOPG
Gaussian broadening (eV)	0.42±0.01	0.43±0.01	0.42±0.01	0.39±0.01
Binding energy (eV)	284.45±0.05	284.45±0.05	284.45±0.05	284.40±0.05
Lorentzian width (eV)	0.28±0.01	0.26±0.01	0.22±0.01	0.10±0.01
FWHM (eV)	0.69±0.05	0.66±0.05	0.64±0.05	0.50±0.05
Singularity index (α)	0.15±0.01	0.15±0.01	0.15±0.01	0.11±0.01

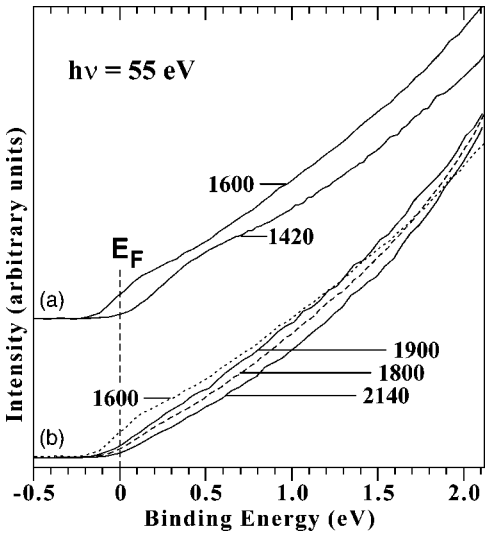

FIG. 6. Evolution of the valance band spectra near the Fermi level (E_F) as a function of annealing temperature for samples annealed at (a) 1420 and 1600 K; (b) 1600, 1800, 1900, and 2140 K (temperatures on the figure are presented in kelvin). Spectra were obtained in normal emission geometry using a photon energy of 55 eV.

prominent peaks at 2.8 ± 0.1 eV and 7.5 ± 0.1 eV and a shoulder at 4.2 ± 0.1 eV. The first peak, at 2.8 ± 0.1 eV, is related to π bonding in graphite.[32,38,62] Progressive graphitization of the ND in samples annealed at 1420 and 1600 K, and the eventual vanishing of sp^3 carbon from the C1*s* photoemission spectra (Fig. 4) in the sample annealed at 1800 K results in increasing intensity and sharpness of the peak at 2.8 ± 0.1 eV in the valence band spectra. The sharpening and increase in intensity of this peak demonstrates increased π bonding with increasing annealing temperature. A similar result was obtained by Diaz *et al.*[49] in their study of the graphitization of amorphous carbon films. This process is accompanied by an increasing intensity in the shoulder at 4.2 ± 0.1 eV in the valence band data, which indicates growth of the population of mixed σ-π states.[32,38] The second peak at 7.5 ± 0.1 eV is related to σ bonding in graphite.[32,38] It should be noted that in our previous work (Ref. 38) for the sample annealed at 2140 K we found positions for π and σ peaks of 2.92 eV and 7.84 eV respectively. The small shift to lower binding energy in these peaks found in this work can be attributed to differences in the pretreatment of the samples: before the measurements of valance band spectra the samples were annealed at 1300 K for 5 minutes in the present work whereas in Ref. 38 samples were annealed at 670 K.

Figure 6(a) shows valence band spectra near the Fermi level of the diamond-containing samples annealed at 1420 and 1600 K. These spectra [and those in Fig. 6(b)] were obtained with higher resolution, better statistics, and smaller step size than those in Fig. 5. We see that graphitization of the samples results in an increase in the density of electronic states at the Fermi level. This is in accord with the significant decrease in the electrical resistivity of these samples: a decrease in resistivity of about 6 orders of magnitude has been previously measured for the sample annealed at 1420 K compared with that annealed at 1600 K (see Table I).[42] Further graphitization of the samples at higher temperatures leads to a decrease in the density of states at the Fermi level [Fig. 6(b)]. However, the process is not monotonic—we observed an increase in density of states at the Fermi level for the sample annealed at 1900 K when compared with the sample annealed at 1800 K.

IV. DISCUSSION

Annealing at temperatures above 1100 K results in complete desorption of oxygen-containing groups—therefore the presence of such groups on samples annealed at 1420 and 1600 K (see Fig. 3) can be explained by the their exposure to atmosphere after annealing. At room temperature ambient oxygen may react with the edges of incomplete graphitic layers, where there are highly reactive dangling bonds; in contrast, the basal surfaces of graphite are relatively inert to oxygen at room temperature.[63] Thus the formation of oxygen-containing groups in these samples clearly indicates that the outer fullerene-like shells are not completely closed. On the other hand, the absence of oxygen-containing groups after exposure to atmosphere for the samples annealed at 1800, 1900, and 2140 K suggests that final closure of the outer fullerene-like shells of OLC occurs at temperatures above 1600 K.

The sp^2 component in the C1*s* core-level spectra of the OLC annealed at 1420 K is shifted by 0.3 eV towards higher binding energy with respect to that for HOPG (Figs. 3 and 4; Tables II and III). To explain this shift, we note that previous HRTEM studies[25,26,43] showed that at lower temperatures of graphitization the first 1–3 graphite layers exfoliating from diamond surfaces merge with these surfaces, possess significant curvature, and contain defects. Graphitization of the smallest ND particles (2–3 nm in diameter) at lower temperatures results in the formation of OLC particles with 2–3 fullerenelike shells with the size of inner shells corresponding to the size of the C_{60} fullerene molecule.[25,26] The significant curvature of graphite layers and fullerene-like character of the small OLC particles formed in the sample annealed at 1420 K result in hybridization states of the carbon atoms in this material being intermediate between sp^2 and sp^3.[64] Thus, we suggest that the large curvature of the graphite layers of OLC prepared at 1420 K causes the shift towards higher binding energy for the sp^2 component of this sample.

The inhomogeneity (presence of graphitic layers with different radii of curvature) and disorder in the graphitic structures present in the sample annealed at 1420 K cause the significant broadening of the C1*s* line from this sample, which is characterized by the largest value of FWHM in comparison with the other samples (compare values in Table II and III). The large curvature of graphite layers in this sample also results in degradation of the *p* orbital overlap compared with planar graphite layers and thus explains the absence of a π plasmon satellite in the C1*s* spectrum [Fig. 3(a)], despite the presence of sp^2 hybridized carbon.

Increasing the annealing temperature results in a rise in the concentration of carbon onions with large radius and consequently a small curvature of the outer fullerenelike shells

(see Fig. 1, the HRTEM image at 1600 K). This is accompanied by a shift of C1*s* line towards a lower binding energy of 284.50 ± 0.05 eV, a significant decrease of the FWHM of the C1*s* line for the samples annealed at 1600 K (see Table II), and the appearance of a π plasmon satellite feature in the C1*s* data.

Samples annealed at temperatures of 1800, 1900, and 2140 K do not evidence any sp^3 hybridized carbon in their C1*s* spectra. The C1*s* peak of the samples has a maximum at 284.45 ± 0.05 eV, which is slightly higher than the value of 284.40 ± 0.05 eV found for HOPG (see Table III and Fig. 4), however, the difference in the position of the C1*s* lines is within experimental error. For these samples we found a large (0.22–0.28 eV) Lorentzian width when compared with HOPG (0.10 ± 0.01 eV) (see Table II). These Lorentzian linewidths are also larger than the width of 0.21 eV for HOPG reported by Sette *et al.*[65] There are several possible reasons for such broadening. The first possibility, is that the Lorentzian linewidth accounts for the lifetime of the C1*s* core hole and, as was shown in Ref. 62, the decay of the C1*s* core hole is a result of a *KLL* Auger process. Since the *L* electrons are valence electrons, the core-hole lifetime depends on the hybridization state of carbon atoms in a sample. Carbon atoms in the OLC samples have intermediate hybridization state between pure sp^3 and sp^2 states, due to curvature of the fullerenelike shells. Thus, we could expect that the presence of a *KLL* Auger process can provide extra or faster decay channels in OLC. However, it was demonstrated that the Lorentzian width for sp^3 carbon is even smaller than that for sp^2 carbon.[65,66] Direct measurements of Lorentzian width of diamond give a value of 0.11 eV.[67] Thus, in analogy, one could expect that the introduction of sp^3 states will introduce "narrowing" rather than a "broadening" as we observed in our experiments. We believe that this mechanism cannot explain our data.

The second possible reason may be related to phonon broadening of spectra. Prince *et al.*[66] suggested that decreased lifetime is not real, and is not due to an initial state effect, but that phonon broadening in the final state gives rise to a non-Gaussian line-shape contribution. The presence of characteristic vibrations in carbon onions, which are different from those in planar graphite, was found in their infrared absorption spectra,[16] and in Raman spectra.[10,23,33] We believe that this is one possible reason behind the broadening of the C1*s* lines associated with sp^2 carbon in OLC.

A third possibility for the increased Lorentzian broadening is the difference in surface and bulk states in graphitic materials. Balasubramanian *et al.*[68] measured C1*s* photoemission spectra of HOPG at several excitation energies between 300 and 350 eV in normal emission geometry with a resolution of 50 meV. The observed increase in Lorentzian width of the core level was explained in terms of the splitting of bulk and surface states in the spectra. It was shown that the C1*s* photoemission line is a doublet with a bulk component situated 120 meV lower in binding energy than the surface component.[68] Recently Smith *et al.*[69] resolved the surface to bulk core-level shift in HOPG using monochromated Al K_a x rays with a total instrumental broadening of 0.42 eV. The value obtained for the shift in this work is 0.46 eV. The authors concluded that the differences between the various other data reported for HOPG arise from a combination of factors including sampling depth, availability of final states, and the specific nature of the HOPG specimens used. In our case, one might expect an even larger splitting of the bulk and surface component in the C1*s* photoemission spectra when compared with HOPG, since the inner fullerenelike shells in OLC have more curvature than surface layers. Thus, the increased Lorentzian width of OLC compared with that of HOPG is likely to be caused by the structural differences between OLC and HOPG. The structural nonuniformity of the OLC samples, namely the presence of graphite layers with different curvature can, we believe, be the underlying cause of the large Gaussian broadening of the spectra from these samples and the different value of the singularity index with respect to that of HOPG (Table III).

Finally, we found that samples annealed at 1600, 1800, and 1900 K show a small increase in density of states at the Fermi level (Fig. 6). A possible reason for this is the presence of defects in the fullerenelike shells of OLC. It was shown that the difference in crystal structures of diamond and graphite results in an accumulation of different types of defects in the graphite curved layers during their formation from diamond carbon (see Fig. 1).[32,43] The defects within the curved layers are five or seven atom rings,[3] "Y" junctions of two basal graphite planes[7,25] or an interstitial plane between two basal planes,[7] and vacancies.[32] The x-ray emission spectroscopy study performed in Ref. 32 revealed an increase in the partial density of states near the π peak of OLC produced at 1600 and 1900 K when compared to OLC produced at 2140 K and HOPG. Quantum-chemical calculations on "holed" carbon cages suggest that this increase is due to the additional contribution of electrons from dangling bonds on zigzag edges. This localization might result from defects in the curved graphitic networks, namely, the holes which appear due to the deficit in surface atoms in ND compared with that required to form an ideal spherical shell of the same diameter.[32] We should also note that defects such as holes, interstitial planes and vacancies formed during the graphitization of ND are situated inside the carbon onions, because, as we showed earlier, the absence of oxygen-containing groups in samples annealed at 1800 and 1900 K indicates that their outer fullerenelike shells are closed. This fact can explain the low sensitivity of photoemission spectroscopy to the presence of such defects and thus the rather subtle, but reproducible, nature of the changes in the valence band spectra close to the Fermi level.

The process of accumulation of defects which accompanies the increase in density of states at the Fermi level was also observed by Díaz *et al.*[49] for graphitization of amorphous carbon films, initially containing sp^3 carbon, in the temperature range of 650–1450 K. However, in contrast to the data presented in Ref. 49, we do not observe a shift in the binding energy of the C1*s* peak of the OLC samples to values below those for HOPG. The sample annealed at 2140 K has the lowest density of states at the Fermi level [Fig. 6(b)]. This indicates a decrease in defect concentration within this sample and leads us to the conclusion that temperatures lower than 1900 K are not sufficiently high enough to make carbon atoms mobile in order to anneal out defects. It is interesting to note that 2140 K is close to the typical range of

temperatures (2200–2400 K) where the process of full graphitization of amorphous carbon occurs.[63,70]

V. CONCLUSIONS

We have studied the products of the high temperature phase transformation of ND by core level and valance band photoemission spectroscopy. The formation of oxygen-containing groups in samples annealed at 1420 and 1600 K and then exposed to air indicates the presence of edges in (incomplete) graphitic layers in these samples. Such oxygen-containing groups were not detected in samples annealed at 1800, 1900, and 2140 K and then exposed to air. Therefore, we suggest that annealing at temperatures higher than 1600 K results in the full closure of the outer fullerenelike shells of OLC. We found a large (0.22–0.28 eV) Lorentzian width for samples annealed at 1800, 1900, and 2140 K when compared with HOPG (0.12 ± 0.01). We propose that the most likely reason for such broadening is a splitting of bulk and surface components in the C1*s* photoemission spectra of OLC. This splitting is larger for OLC, when compared with HOPG, since the inner fullerenelike shells in OLC have more curvature than the planar HOPG layers. The 0.30 ± 0.05 eV and 0.10 ± 0.05 eV shifts to higher binding energy of the sp^2 carbon component of the C1*s* lines for the samples annealed at 1420 K and 1600 K, respectively, when compared with the binding energy of the sp^2 component of HOPG were explained by the significant curvature of graphite layers of the small OLC particles formed during initial graphitization. An increase in density of states near the Fermi level is caused by an accumulation of different types of defects in the curved graphite layers during graphitization of nanodiamond up to a temperature of 1900 K. Annealing at higher temperatures resulted in healing of these defects and was reflected in a decrease in density of states at the Fermi level.

ACKNOWLEDGMENTS

Y.B. is grateful to the Royal Society for financial support. L.Š. would like to thank the Royal Society and EPSRC (GR/A92200/01) for financial support. S.K. thanks the scholarship panel of the University of Newcastle upon Tyne for financial support. A.K.C. acknowledges financial support from the EPSRC and the University of Nottingham. We thank G. Miller for valuable technical support during the experiment.

*Corresponding author. Email addresses: yuriy.butenko@newcastle.ac.uk, butenko@catalysis.nsk.su

[1] S. Iijima, J. Cryst. Growth **50**, 675 (1980).
[2] D. Ugarte, Nature (London) **359**, 707 (1992).
[3] H. Terrones and M. Terrones, J. Phys. Chem. Solids **58**, 1789 (1997).
[4] H. W. Kroto, Nature (London) **359**, 670 (1992).
[5] F. Banhart, and P. M. Ajayan, Nature (London) **382**, 433 (1996).
[6] V. V. Roddatis, V. L. Kuznetsov, Yu. V. Butenko, D. S. Su, and R. Schlögl, Phys. Chem. Chem. Phys. **4**, 1964 (2002).
[7] F. Banhart, Rep. Prog. Phys. **62**, 1181 (1999).
[8] T. Stöckli, J.-M. Bonard, A. Châtelain, Z. L. Wang, and P. Stadelmann, Phys. Rev. B **61**, 5751 (2000).
[9] W. A. de Heer and D. Ugarte, Chem. Phys. Lett. **207**, 480 (1993).
[10] W. S. Bacsa, W. A. de Heer, D. Ugarte, and A. Châtelain, Chem. Phys. Lett. **211**, 283 (1993).
[11] T. Cabioc'h, J. P. Riviere, and J. Delafond, J. Mater. Sci. **30**, 4787 (1995).
[12] T. Cabioch, J. C. Girard, M. Jaouen, M. F. Denanot, and G. Hug, Europhys. Lett. **38**, 471 (1997).
[13] T. Cabioc'h, M. Jaouen, M. F. Denanot, and P. Bechet, Appl. Phys. Lett. **73**, 3096 (1998).
[14] T. Cabioc'h, T. E. Thune, J. P. Riviere, S. Camelio, J. C. Girard, P. Guerin, M. Jaouen, L. Henrard, and Ph. Lambin, J. Appl. Phys. **91**, 1560 (2002).
[15] T. Pichler, M. Knupfer, M. S. Golden, J. Fink, and T. Cabioc'h, Phys. Rev. B **63**, 155415 (2001).
[16] T. Cabioc'h, A. Kharbach, A. Le Roy, and J. P. Riviere, Chem. Phys. Lett. **285**, 216 (1998).
[17] T. Cabioc'h, S. Camelio, L. Henrard, and Ph. Lambin, Eur. Phys. J. B **18**, 535 (2000).
[18] M. Kociak, L. Henrard, O. Stéphan, K. Suenaga, and C. Colliex, Phys. Rev. B **61**, 13 936 (2000).
[19] L. Henrard, F. Malengreau, P. Rudolf, K. Hevesi, R. Caudano, P. Lambin, and T. Cabioc'h, Phys. Rev. B **59**, 5832 (1999).
[20] N. Sano, H. Wang, M. Chhowalla, I. Alexandrou, and G. A. Amaratunga, Nature (London) **414**, 506 (2001).
[21] N. Sano, H. Wang, I. Alexandrou, M. Chhowalla, K. B. K. Teo, G. A. J. Amaratunga, and K. Iimura, J. Appl. Phys. **92**, 2783 (2002).
[22] I. Alexandrou, H. Wang, N. Sano, and G. A. J. Amaratunga, J. Chem. Phys. **120**, 1055 (2004).
[23] D. Roy, M. Chhowalla, H. Wang, N. Sano, I. Alexandrou, T. W. Clyne, and G. A. J. Amaratunga, Chem. Phys. Lett. **373**, 52 (2003).
[24] M. Chhowalla, H. Wang, N. Sano, K. B. K. Teo, S. B. Lee, and G. A. J. Amaratunga, Phys. Rev. Lett. **90**, 155504 (2003).
[25] V. L. Kuznetsov, A. L. Chuvilin, Yu. V. Butenko, and V. M. Titov, Chem. Phys. Lett. **222**, 343 (1994).
[26] Yu. V. Butenko, V. L. Kuznetsov, A. L. Chuvilin, V. N. Kolomiichuk, S. V. Stankus, R. A. Khairulin, and B. Segall, J. Appl. Phys. **88**, 4380 (2000).
[27] A. S. Barnard, S. P. Russo, and I. K. Snook, Phys. Rev. B **68**, 073406 (2003).
[28] J.-Y. Raty, G. Galli, C. Bostedt, T. W. van Buuren, and L. J. Terminello, Phys. Rev. Lett. **90**, 037401 (2003).
[29] D. Ugarte, Carbon **32**, 1245 (1994).
[30] E. Koudoumas, O. Kokkinaki, M. Konstantaki, S. Couris, S. Korovin, P. Detkov, V. Kuznetsov, S. Pimenov, and V. Pustovoi, Chem. Phys. Lett. **357**, 336 (2002).
[31] N. Keller, N. I. Maksimova, V. V. Roddatis, M. Schur, G. Mestl, V. L. Kuznetsov, Yu. V. Butenko, and R. Schlögl, Angew.

Chem., Int. Ed. **41**, 1885 (2002).
[32] A. V. Okotrub, L. G. Bulusheva, V. L. Kuznetsov, Yu. V. Butenko, A. L. Chuvilin, and M. I. Heggie, J. Phys. Chem. A **105**, 9781 (2001).
[33] E. D. Obraztsova, M. Fujii, S. Hayashi, V. L. Kuznetsov, Yu. V. Butenko, and A. L. Chuvilin, Carbon **36**, 821 (1998).
[34] S. Tomita, M. Fujii, S. Hayashi, and K. Yamamoto, Chem. Phys. Lett. **305**, 225 (1999).
[35] S. Tomita, T. Sakurai, H. Ohta, M. Fujii, and S. Hayashi, J. Chem. Phys. **114**, 7477 (2001).
[36] S. Tomita, A. Burian, J. C. Dore, D. LeBolloch, M. Fujii, and S. Hayashi, Carbon **40**, 1469 (2002).
[37] S. Tomita, S. Hayashi, Y. Tsukuda, and M. Fujii, Phys. Solid State **44**, 450 (2002).
[38] M. Montalti, S. Krishnamurthy, Y. Chao, Yu. V. Butenko, V. L. Kuznetsov, V. R. Dhanak, M. R. C. Hunt, and L. Siller, Phys. Rev. B **67**, 113401 (2003).
[39] V. L. Kuznetsov, A. L. Chuvilin, E. M. Moroz, V. N. Kolomiichuk, S. K. Shaikhutdinov, Yu. V. Butenko, and I. Yu. Malkov, Carbon **32**, 873 (1994).
[40] S. Doniach, and M. Šunjič, J. Phys. C **3**, 285 (1970).
[41] D. A. Shirley, Phys. Rev. B **5**, 4709 (1972).
[42] V. L. Kuznetsov, Yu. V. Butenko, A. L. Chuvilin, A. I. Romanenko, and A. V. Okotrub, Chem. Phys. Lett. **336**, 397 (2001).
[43] V. L. Kuznetsov, I. L. Zilberberg, Yu. V. Butenko, A. L. Chuvilin, and B. Segall, J. Appl. Phys. **86**, 863 (1999).
[44] V. L. Kuznetsov, A. L. Chuvilin, Yu. V. Butenko, A. K. Gutakovskii, S. V. Stankus, and R. A. Khairulin, Chem. Phys. Lett. **289**, 353 (1998).
[45] H. W. Kroto and K. McKay, Nature (London) **331**, 328 (1988).
[46] M. Ozawa, H. Goto, M. Kusunoki, and E. Ōsawa, J. Phys. Chem. B **106**, 7135 (2002).
[47] J. I. B. Wilson, J. S. Walton, and G. Beamson, J. Electron Spectrosc. Relat. Phenom. **121**, 183 (2001).
[48] V. L. Kuznetsov and Yu. V. Butenko, in *Nanostructured Materials and Coatings for Biomedical and Sensor Applications*, edited by Y. G. Gogotsi and I. V. Uvarova, NATO Science Series (Kluwer Academic, Dordrecht 2003), p. 187.
[49] J. Díaz, G. Paolicelli, S. Ferrer, and F. Comin, Phys. Rev. B **54**, 8064 (1996).
[50] P. A. Brühwiler, A. J. Maxwell, C. Puglia, A. Nilsson, S. Andersson, and N. Mårtensson, Phys. Rev. Lett. **74**, 614 (1995).
[51] Y. Mizokawa, T. Miyasato, S. Nakamura, K. M. Geib, and C. W. Wilmsen, J. Vac. Sci. Technol. A **5**, 2809 (1987).
[52] A. B. Christie, in *Methods of Surface Analysis. Techniques and Applications*, edited by J. M. Walls (Cambridge University Press, Cambridge, England, 1989), p. 127.
[53] D. Pantea, H. Darmstadt, S. Kaliaguine, and C. Roy, Appl. Surf. Sci. **217**, 181 (2003).
[54] S. D. Gardner, C. S. K. Singamsetty, G. L. Booth, G.-R. He, and C. U. Pittman Jr., Carbon **33**, 587 (1995).
[55] U. Zielke, K. J. Hüttinger, and W. P. Hoffman, Carbon **34**, 983 (1996).
[56] S. Biniak, G. Szymański, J. Siedlewski, and A. Światkowski, Carbon **35**, 1799 (1997).
[57] C. Moreno-Castilla, M. V. López-Ramón, and F. Carrasco-Marín, Carbon **38**, 1995 (2000).
[58] K. Shibagaki and S. Motojima, Carbon **38**, 2087 (2000).
[59] R. Haerle, E. Riedo, A. Pasquarello, and A. Baldereschi, Phys. Rev. B **65**, 045101 (2002).
[60] P. Mérel, M. Tabbal, M. Chaker, S. Moisa, and J. Margot, Appl. Surf. Sci. **136**, 105 (1998).
[61] J. Fink, Th. Müller-Heinzerling, J. Pflüger, B. Scheerer, B. Dischler, P. Koidl, A. Bubenzer, and R. E. Sah, Phys. Rev. B **30**, 4713 (1984).
[62] P. Skytt, P. Glans, D. C. Mancini, J.-H. Guo, N. Wassdahl, J. Nordgren, and Y. Ma, Phys. Rev. B **50**, 10 457 (1994).
[63] R. Schlögl, in *Handbook of Heterogeneous Catalysis*, edited by G. Ertl, H. Knözinger, and J. Weitkamp (Wiley-VCH, Weinheim, 1997), Vol. 1, p. 138.
[64] R. C. Haddon and K. Raghavachari, in *Buckminsterfullerenes*, editied by W. E. Billups and Marco A. Ciufolini (Wiley, New York, 1993), Chap. 7.
[65] F. Sette, G. K. Wertheim, Y. Ma, G. Meigs, S. Modesti, and C. T. Chen, Phys. Rev. B **41**, 9766 (1990).
[66] K. C. Prince, I. Ulrych, M. Peloi, B. Ressel, V. Chab, C. Crotti, and C. Comicioli, Phys. Rev. B **62**, 6866 (2000).
[67] K. A. Mäder, and S. Baroni, Phys. Rev. B **55**, 9649 (1997).
[68] T. Balasubramanian, J. N. Andersen, and L. Wallden, Phys. Rev. B **64**, 205420 (2001).
[69] R. A. P. Smith, C. W. Armstrong, G. C. Smith, and P. Weightman, Phys. Rev. B **66**, 245409 (2002).
[70] J. N. Rouzand and A. Oberlin, Carbon **27**, 517 (1989).